JOURNAL OF MOLECULAR SPECTROSCOPY 122, 440–454 (1987)

The Far-Infrared Laser Magnetic Resonance Spectrum of the ^{17}OH Radical: Determination of Nuclear Hyperfine Parameters[1]

KENNETH R. LEOPOLD AND KENNETH M. EVENSON

Time and Frequency Division, National Bureau of Standards, Boulder, Colorado 80303

AND

ELIZABETH R. COMBEN AND JOHN M. BROWN

The Physical Chemistry Laboratory, South Parks Road, Oxford OX1 3QZ, England

The far-infrared (FIR) Laser Magnetic Resonance (LMR) spectrum of the ^{17}OH radical in the $v = 0$ level of the $X^2\Pi$ state has been studied in detail. The measurements have been analyzed and, in combination with some earlier EPR measurements, subjected to a single least-squares fit using an effective Hamiltonian. A full set of ^{17}O nuclear hyperfine parameters has been determined. Some implications of these parameter values for the electronic wavefunction of OH are considered.

1. INTRODUCTION

The hydroxyl radical has played a leading role in free radical chemistry and spectroscopy for a long time. That it still holds this position today is evident from current interest in its involvement in the interstellar medium (*1*) and atmospheric chemistry (*2*). From the spectroscopic standpoint, it was the first short-lived free radical to be detected in the microwave region (*3*). In the intervening years, a large number of studies have been made such that almost every conceivable type of transition between the levels of ^{16}OH in its ground $^2\Pi$ state has now been detected. Very recently, for example, transitions between individual spin–rotation levels of the molecule were detected at zero magnetic field by tunable far-infrared spectroscopy (*4*, *5*). Isotopic modifications of OH have also been studied quite thoroughly. Details of this work can be obtained from the references in recent spectroscopic papers on OD (*6*) and ^{18}OH (*7*).

In the present paper, we are concerned with another isotopic variant, ^{17}OH. Our primary objective is a complete determination of the ^{17}O hyperfine parameters so that we can learn more about the electronic wavefunction in the region of the oxygen nucleus. Unlike the corresponding region around the proton, this part of the wavefunction is comparatively poorly characterized. The first recorded study of ^{17}OH appears to be that made by Ehrenstein (*8*) in the microwave region. He generated the free radical by passing an electric discharge through H_2 ^{17}O and detected four hyperfine

[1] Work supported in part by NASA Contract W-15, 047.

0022-2852/87 $3.00

components of the $J = \frac{7}{2}$, F_1 ($\simeq {}^2\Pi_{3/2}$) lambda-doubling transition at 13.3 GHz. From this, he was able to determine the value for one hyperfine parameter, d. The next investigation was by Carrington and Lucas who studied the lambda-doubling transitions in the $J = \frac{3}{2}$ level of the F_1 spin component by gas phase EPR (*9*). They interpreted their results in terms of three magnetic hyperfine parameters and one electric quadrupole coupling constant. Further measurements were made on the microwave spectrum of ^{17}OH by Gottlieb *et al.* (*10*). They generated ^{17}OH by the reaction of H atoms with $N^{17}O_2$, and their measurements related to lambda-doubling transitions in the $J = \frac{3}{2}$ and $\frac{5}{2}$ levels of the F_1 component and to the $J = \frac{1}{2}$ level. No quantitative analysis of their results has been performed. Finally, microwave transitions in ^{17}OH have also been detected in the interstellar medium by Gardner and Whiteoak (*11*). In this case, the observation was restricted to a proton hyperfine doublet which was assigned to the $J = \frac{3}{2}$ transition on the basis of calculations by Valtz and Soglasnova (*12*). The same transitions had actually been measured more precisely in the laboratory study (*10*).

In the present paper, we describe the observation and analysis of lines in the laser magnetic resonance spectrum of ^{17}OH at far-infrared wavelengths. Four transitions have been studied in this way. Two are pure rotational transitions and the other two are fine structure transitions between the two spin components. The observations are summarized in Table I and also in the energy-level diagram of Fig. 1. An attempt was made to analyze the microwave measurements (*10*) and the present data simultaneously. These calculations revealed inconsistencies between the two data sets which, despite our best efforts, we have been unable to reconcile. The microwave spectrum of ^{17}OH is currently being reinvestigated by Drs. Gottlieb and Radford (*13*) to check the tentative assignments of the microwave frequencies given in Ref. (*10*). It may be that some of the frequencies quoted are associated with a species other than ^{17}OH. In view of these uncertainties, we have confined our analysis to the EPR (*9*) and LMR data. In addition to obtaining reliable values for the rotational and spin–orbit coupling constants, we have achieved the first full determination of the ^{17}O hyperfine parameters for ^{17}OH.

TABLE I

Summary of Observations in the Far-Infrared LMR Spectrum of the ^{17}OH Radical in Its Ground State

Laser line				^{17}OH transition	
Pump	Gain medium	$\lambda/\mu m$	ν/GHz	J	F_i
9P(22)	$^{13}CH_3OH$	85.3	3513.8530	$3\frac{1}{2} \leftarrow 2\frac{1}{2}$	$F_1 \leftarrow F_1$
9R(10)	CH_3OH	96.5	3105.9368	$1\frac{1}{2} \leftarrow 2\frac{1}{2}$	$F_2 \leftarrow F_1$
10R(16)	$^{13}CH_3OH$	115.8	2588.3617	$2\frac{1}{2} \leftarrow 3\frac{1}{2}$	$F_2 \leftarrow F_1$
9P(36)	CH_3OH	118.8	2522.7816	$2\frac{1}{2} \leftarrow 1\frac{1}{2}$	$F_1 \leftarrow F_1$
10R(36)	CD_2F_2	120.5	2488.5534	$2\frac{1}{2} \leftarrow 1\frac{1}{2}$	$F_1 \leftarrow F_1$

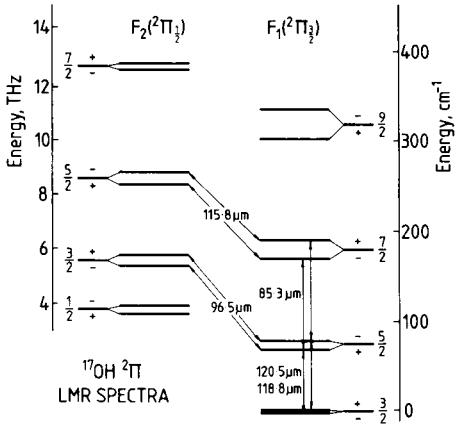

FIG. 1. Energy-level diagram showing the lower rotational levels of ^{17}OH in the $v = 0$ level of the $X^2\Pi$ state and the transitions studied by far-infrared LMR spectroscopy in the present work. The lambda-doubling intervals are exaggerated by a factor of 20 for the sake of clarity.

2. EXPERIMENTAL DETAILS

The LMR apparatus used to detect ^{17}OH has been described elsewhere in detail (*14*). Briefly, it consists of a far-infrared gain cell which is transversely pumped by a grating-tuned carbon dioxide laser. The FIR laser gas is separated from the intracavity sample region by a polypropylene beam splitter mounted at Brewster's angle with respect to the laser cavity axis. The sample region is situated between the ring-shimmed 38-cm pole caps of an electromagnet which produces a homogeneous field region 7.5 cm in diameter. A small part of the circulating laser power is reflected out of the cavity by a movable 45° copper mirror and is monitored as a function of magnetic field strength by a gallium-doped germanium bolometer at about 1.5 K. The rotating coil magnetometer used to stabilize the magnetic field was calibrated intermittently with a proton NMR gaussmeter. Magnetic flux measurements had an overall uncertainty of 10^{-5} T below 0.1 T and a fractional uncertainty of 10^{-4} T above this field strength. Infrared laser frequencies (see Table I) were taken from the recent review of Inguscio *et al.* (*15*) and are considered accurate to 3×10^{-7} of the laser frequency.

The OH radicals were produced by the reaction of nitrogen dioxide with H atoms formed in a 2450-MHz discharge through H_2O or a H_2O/H_2 mixture in helium. Flame conditions were optimized on convenient ^{16}OH transitions before proceeding to the lines of ^{17}OH which were observed in natural abundance (0.037%). Spectra were recorded at a total pressure of between 27 and 100 Pa (1 Torr ≡ 133.32 Pa). Figure 2 shows a recording of part of the $J = 2\frac{1}{2} \leftarrow 1\frac{1}{2}$, F_1 transition of ^{17}OH which clearly shows the 12-line hyperfine pattern expected for this species (six transitions associated with the spin of $\frac{5}{2}$ for ^{17}O each split into a doublet by the ^1H hyperfine interaction). Magnetic flux densities and quantum number assignments for all the measured Zeeman components are given in Table II. This list is comprehensive but not exhaustive; in places, for example, the ^{17}OH lines were completely swamped by the much stronger ^{16}OH transitions.

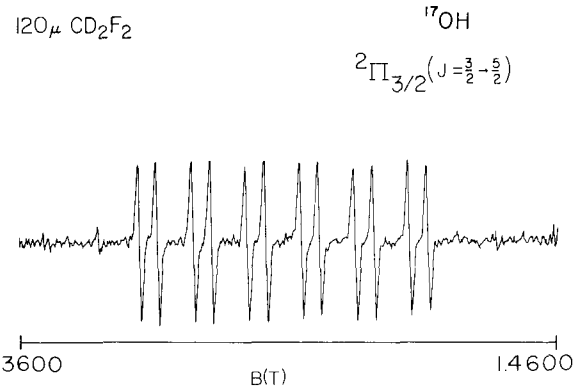

FIG. 2. Part of the far-infrared LMR spectrum of the ^{17}OH radical recorded with the 120.5-μm line in parallel polarization. The OH transition involved is $^2\Pi_{3/2}$, $J = \frac{5}{2} \leftarrow \frac{3}{2}$, $+ \leftarrow -$, $M_J = \frac{3}{2} \leftarrow \frac{3}{2}$. The six-line pattern arises from ^{17}O hyperfine interactions ($I = \frac{5}{2}$). Each of these transitions is further split into a doublet from the proton hyperfine interaction. The spectrum was recorded with ^{17}O in natural abundance (0.037%) with a 300-msec output time constant. The signal-to-noise ratio for the corresponding transition in ^{16}OH would be 2×10^5 to 1 (see the text for details).

3. ANALYSIS

3.1. Assignments

The assignments of quantum numbers to the various observed lines was a straightforward process. They were made by comparison of the experimental spectra with the predictions of a computer program which has been described in some detail elsewhere (*16*). This program predicts the fields and relative intensities of Zeeman transitions between selected rotational levels resonant with a particular laser frequency. The values for ^{17}OH in the $v = 0$ level of the $X^2\Pi$ state required for this calculation were obtained by the isotopic scaling of the corresponding parameter set for ^{16}OH (*17*). This led to quite unambiguous assignments which are given in Table II.

3.2. Least-Squares Fit

The measurements listed in Table II were used with the EPR measurements of Ref. (*9*) to determine appropriate molecular parameters in the effective Hamiltonian for ^{17}OH:

$$\mathscr{H}_{\text{eff}} = \mathscr{H}_{\text{so}} + \mathscr{H}_{\text{rot}} + \mathscr{H}_{\text{cd}} + \mathscr{H}_{\text{LD}} + \mathscr{H}_{\text{sr}} + \mathscr{H}_{\text{hfs}} + \mathscr{H}_{\text{Q}} + \mathscr{H}_{\text{Zeem}}. \quad (1)$$

This Hamiltonian, which has been described in detail elsewhere (*16*), was used in previous fits of OH data (*6, 7, 17*). The rotationally dependent terms in the Hamiltonian are formulated in terms of $\mathbf{N}^2$ rather than $\mathbf{R}^2$ (*18*). The basis set was truncated without any loss in accuracy at matrix elements with $\Delta J = \pm 1$. Each datum was weighted in the fit, inversely as the square of the experimental uncertainty (which for the LMR data arises primarily from the knowledge of the laser frequency as used in the experiment).

The present data set is not adequate for the determination of all the parameters in the molecular Hamiltonian. Several of the parameters were therefore constrained to

TABLE II

Flux Densities and Frequencies of Transitions Observed by LMR for ^{17}OH in the $X^2\Pi$ State

Parity[a]	M_J'[b]	M_{I_1}'	M_{I_2}'	M_J	M_{I_1}	M_{I_2}	Flux density (G)	$\nu_{laser}-\nu_{calc}$[c] (MHz)	Tuning rate (MHz/G)
85.3 μm spectrum (ν_L = 3513853.0 MHz) ; $F_1, J = 3\frac{1}{2} \leftarrow F_1, J = 2\frac{1}{2}$									
Perpendicular polarisation (σ)									
+	1½	-2½	½	2½	-2½	½	17768.66	-5.2	-1.02
+	1½	-2½	-½	2½	-2½	-½	17785.58	-2.0	-1.02
+	1½	-1½	½	2½	-1½	½	17855.29	-1.4	-1.02
+	1½	-1½	-½	2½	-1½	-½	17871.02	0.7	-1.02
+	1½	-½	½	2½	-½	½	17939.12	0.5	-1.02
+	1½	-½	-½	2½	-½	-½	17952.84	0.5	-1.02
+	1½	½	½	2½	½	½	18022.25	2.6	-1.02
+	1½	½	-½	2½	½	-½	18035.87	2.4	-1.02
+	1½	1½	½	2½	1½	½	18100.67	0.6	-1.02
+	1½	1½	-½	2½	1½	-½	18114.89	1.1	-1.02
+	1½	2½	½	2½	2½	½	18179.99	0.5	-1.02
+	1½	2½	-½	2½	2½	-½	18193.11	-0.2	-1.02
96.5 μm spectrum (ν_L = 3105936.8 MHz) ; $F_2, J = 1\frac{1}{2} \leftarrow F_1, J = 2\frac{1}{2}$									
Perpendicular polarisation (σ)									
+	1½	-2½	+½	2½	-2½	½	3323.4	1.9	-1.97
+	1½	-2½	-½	2½	-2½	-½	3323.4	-1.3	-1.97
+	1½	-½	+½	2½	-½	½	3543.9	0.8	-1.96
+	1½	-½	-½	2½	-½	-½	3543.9	-2.6	-1.96
+	1½	½	+½	2½	½	½	3662.7	1.1	-1.96
+	1½	½	-½	2½	½	-½	3662.7	-2.3	-1.96
+	1½	2½	+½	2½	2½	½	3920.8	3.1	-1.98
+	1½	2½	-½	2½	2½	-½	3920.8	-0.1	-1.98
-	1½	-2½	½	2½	-2½	½	4866.2	-1.7	-1.79
-	1½	-2½	-½	2½	-2½	-½	4866.2	5.1	-1.79
-	1½	-1½	½	2½	-1½	½	4924.2	-0.8	-1.79
-	1½	-1½	-½	2½	-1½	-½	4924.2	5.3	-1.79
-	1½	-½	½	2½	-½	½	4979.6	-1.3	-1.79
-	1½	-½	-½	2½	-½	-½	4979.6	4.5	-1.79
-	1½	½	½	2½	½	½	5036.9	-1.8	-1.79
-	1½	½	-½	2½	½	-½	5036.9	3.8	-1.79
-	1½	1½	½	2½	1½	½	5097.9	-0.6	-1.79
-	1½	1½	-½	2½	1½	-½	5097.9	5.0	-1.79

[a] Parity of lower state.

[b] Primed quantum numbers refer to the upper state.

[c] Calculated frequency obtained using the parameter values from Table IV.

TABLE II—*Continued*

Parity[a]	M_J'[b]	M_{I_1}'	M_{I_2}'	M_J	M_{I_1}	M_{I_2}	Flux density (G)	$\nu_{laser}-\nu_{calc}$[c] (MHz)	Tuning rate (MHz/G)
96.5 μm spectrum (ν_L = 3105936.8 MHz) ; F_2,J = 1½ ← F_1,J = 2½ contd.									
Perpendicular polarisation (σ)									
+	½	-2½	½	1½	-2½	½	6206.5	4.4	-1.10
+	½	-2½	-½	1½	-2½	-½	6206.5	-0.2	-1.10
+	½	-1½	½	1½	-1½	½	6304.6	2.4	-1.10
+	½	-1½	-½	1½	-1½	-½	6304.6	-2.2	-1.10
+	½	-½	½	1½	-½	½	6408.3	3.0	-1.10
+	½	-½	-½	1½	-½	-½	6408.3	-1.6	-1.10
+	½	½	½	1½	½	½	6515.3	3.0	-1.10
+	½	½	-½	1½	½	-½	6515.3	-1.5	-1.10
+	½	1½	½	1½	1½	½	6626.9	3.5	-1.10
+	½	1½	-½	1½	1½	-½	6626.9	-1.0	-1.10
+	½	2½	½	1½	2½	½	6742.6	2.9	-1.11
+	½	2½	-½	1½	2½	-½	6742.6	-1.5	-1.11
-	½	-2½	½	1½	-2½	½	8021.0	-3.2	-1.08
-	½	-2½	-½	1½	-2½	-½	8021.0	4.2	-1.08
Parallel polarisation (π)									
+	1½	-½	-½	1½	-½	-½	5441.7	0.7	-1.29
+	1½	-½	½	1½	-½	½	5441.7	-0.7	-1.29
+	1½	½	-½	1½	½	-½	5584.6	0.7	-1.29
+	1½	½	½	1½	½	½	5584.6	-0.7	-1.29
+	1½	1½	-½	1½	1½	-½	5733.8	0.8	-1.29
+	1½	1½	½	1½	1½	½	5733.8	-0.5	-1.29
+	1½	2½	-½	1½	2½	-½	5889.9	1.3	-1.29
+	1½	2½	½	1½	2½	½	5889.9	-0.2	-1.29
-	1½	2½	-½	1½	2½	-½	6670.7	-0.4	-1.29
-	1½	2½	½	1½	2½	½	6704.2	-0.4	-1.29
-	1½	1½	-½	1½	1½	-½	6729.2	0.6	-1.28
-	1½	1½	½	1½	1½	½	6760.9	-1.7	-1.28
-	1½	½	-½	1½	½	-½	6798.8	0.3	-1.28
-	1½	½	½	1½	½	½	6831.3	-0.3	-1.28
-	1½	-½	-½	1½	-½	-½	6883.6	-0.0	-1.27
-	1½	-½	½	1½	-½	½	6916.1	0.1	-1.27
-	1½	-1½	-½	1½	-1½	-½	6990.7	2.5	-1.27
-	1½	-1½	½	1½	-1½	½	7020.9	0.1	-1.27
-	1½	-2½	-½	1½	-2½	-½	7121.4	-1.6	-1.27
-	1½	-2½	½	1½	-2½	½	7155.0	0.2	-1.27

TABLE II—*Continued*

Parity[a]	M_J'[b]	M_{I_1}'	M_{I_2}'	M_J	M_{I_1}	M_{I_2}	Flux density (G)	$\nu_{laser}-\nu_{calc}$[c] (MHz)	Tuning rate (MHz/G)
96.5 μm spectrum (ν_L = 3105936.8 MHz) ; $F_2, J = 1\frac{1}{2} \leftarrow F_1, J = 2\frac{1}{2}$ contd.									
Parallel polarisation (π)									
+	½	-2½	½	½	-2½	½	16666.7	-10.3	-0.407
+	½	-2½	-½	½	-2½	-½	16666.7	-10.9	-0.407
+	½	-1½	½	½	-1½	½	16814.8	-9.7	-0.407
+	½	-1½	-½	½	-1½	-½	16814.8	-10.4	-0.407
+	½	-½	½	½	-½	½	16966.8	-9.4	-0.407
+	½	-½	-½	½	-½	-½	16966.8	-10.1	-0.407
+	½	½	½	½	½	½	17122.8	-9.5	-0.407
+	½	½	-½	½	½	-½	17122.8	-10.1	-0.407
+	½	1½	½	½	1½	½	17285.3	-8.9	-0.407
+	½	1½	-½	½	1½	-½	17285.3	-9.5	-0.407
+	½	2½	½	½	2½	½	17451.8	-8.9	-0.407
+	½	2½	-½	½	2½	-½	17451.8	-9.5	-0.407
115.8 μm spectrum (ν_L = 2588361.7 MHz) ; $F_2, J = 2\frac{1}{2} \leftarrow F_1, J = 3\frac{1}{2}$									
Perpendicular polarisation (σ)									
+	2½	2½	-½	3½	2½	-½	5991.4	-10.8	-2.07
+	2½	½	½	3½	½	½	6076.3	-0.1	-2.06
+	2½	-1½	-½	3½	-1½	-½	6076.3	-7.7	-2.06
+	2½	-1½	½	3½	-1½	½	6107.7	-2.5	-2.06
+	2½	-2½	-½	3½	-2½	-½	6123.8	0.9	-2.06
+	2½	-2½	½	3½	-2½	½	6152.2	-0.2	-2.06
-	2½	-2½	-½	3½	-2½	-½	8215.0	-1.1	-2.08
-	2½	-2½	+½	3½	-2½	½	8225.4	-0.2	-2.08
-	2½	-1½	-½	3½	-1½	-½	8326.8	-1.6	-2.08
-	2½	-1½	½	3½	-1½	½	8444.4	6.8	-2.08
-	2½	-½	½	3½	-½	½	8454.3	6.6	-2.08
-	2½	½	-½	3½	½	-½	8555.5	-1.6	-2.08
-	2½	½	½	3½	½	½	8564.9	-2.8	-2.08
-	2½	1½	-½	3½	1½	-½	8673.1	0.2	-2.08
-	2½	1½	½	3½	1½	½	8682.9	-0.1	-2.08
-	2½	2½	-½	3½	2½	-½	8791.0	-0.6	-2.08
-	2½	2½	½	3½	2½	½	8801.3	-0.1	-2.08

values estimated from the corresponding values for ^{16}OH with the use of appropriate isotopic scaling factors. Parameters have been determined for ^{16}OH in previous work (*16, 17*). However, an additional but important measurement on the Zeeman effect of ^{16}OH in the $J = \frac{1}{2}$ level has recently been reported by Van Herpen *et al.* (*19*). We have therefore taken the opportunity to incorporate these data into the fit described

TABLE II—*Continued*

Parity[a]	M_J'[b]	M_{I_1}'	M_{I_2}'	M_J	M_{I_1}	M_{I_2}	Flux density (G)	$\nu_{laser}-\nu_{calc}$[c] (MHz)	Tuning rate (MHz/G)
118.8 μm spectrum (ν_L = 2522781.6 MHz) ; F_1,J = 2½ ← F_1,J = 1½									
Perpendicular polarisation (σ)									
+	-½	-2½	½	-1½	-2½	½	9970.7	0.9	1.62
+	-½	-2½	-½	-1½	-2½	-½	9994.7	-1.0	1.62
+	-½	-1½	½	-1½	-1½	½	10064.2	-0.5	1.62
+	-½	-1½	-½	-1½	-1½	-½	10087.9	-0.0	1.62
+	-½	-½	½	-1½	-½	½	10158.2	-0.4	1.62
+	-½	-½	-½	-1½	-½	-½	10182.2	-0.4	1.62
+	-½	½	½	-1½	½	½	10252.3	0.0	1.62
+	-½	½	-½	-1½	½	-½	10276.3	0.0	1.62
+	-½	1½	½	-1½	1½	½	10347.0	-0.2	1.62
+	-½	1½	-½	-1½	1½	-½	10371.1	-0.3	1.62
+	-½	2½	½	-1½	2½	½	10442.0	-0.5	1.62
+	-½	2½	-½	-1½	2½	-½	10465.9	-0.4	1.62
Parallel polarisation (π)									
+	-1½	-2½	½	-1½	-2½	½	17277.9	-4.8	0.946
+	-1½	-2½	-½	-1½	-2½	-½	17312.6	-4.8	0.946
+	-1½	-1½	½	-1½	-1½	½	17375.1	-4.5	0.946
+	-1½	-1½	-½	-1½	-1½	-½	17409.4	-4.2	0.946
+	-1½	-½	½	-1½	-½	½	17468.0	-0.3	0.946
+	-1½	-½	-½	-1½	-½	-½	17501.7	0.6	0.946
+	-1½	½	½	-1½	½	½	17565.0	-0.0	0.946
+	-1½	½	-½	-1½	½	-½	17601.2	-1.5	0.946
+	-1½	1½	½	-1½	½	½	17661.1	1.0	0.946
+	-1½	1½	-½	-1½	1½	-½	17696.6	0.2	0.946
+	-1½	2½	½	-1½	2½	½	17759.1	0.0	0.946
+	-1½	2½	-½	-1½	2½	-½	17793.8	0.0	0.946
120.5 μm spectrum (ν_L = 2488553.4 MHz) ; F_1,J = 2½ ← F_1,J = 1½									
Perpendicular polarisation (σ)									
-	½	-2½	½	1½	-2½	½	7956.79	-1.0	-1.62
-	½	-2½	-½	1½	-2½	-½	7979.40	-1.5	-1.62
-	½	-1½	½	1½	-1½	½	8044.71	-1.1	-1.62
-	½	-1½	-½	1½	-1½	-½	8068.01	-0.5	-1.62
-	½	-½	½	1½	-½	½	8133.02	-1.3	-1.62
-	½	-½	-½	1½	-½	-½	8156.57	-0.2	-1.62
-	½	½	½	1½	½	½	8221.93	-1.1	-1.62

in Ref. (*17*) to determine an improved set of molecular parameters. The main results are given in Table III; further details are given elsewhere (*20*). For the most part, the parameter values are only slightly altered. However, it should be noted that the value

TABLE II—*Continued*

Parity[a]	M_J' [b]	M_{I_1}'	M_{I_2}'	M_J	M_{I_1}	M_{I_2}	Flux density (G)	$\nu_{laser}-\nu_{calc}$ [c] (MHz)	Tuning rate (MHz/G)
120.5 μm spectrum (ν_L = 2488553.4 MHz) ; F_1, J = 2½ ← F_1, J = 1½ contd.									
Perpendicular polarisation (σ)									
-	½	½	-½	1½	½	-½	8244.74	-1.3	-1.62
-	½	1½	½	1½	1½	½	8311.74	-0.0	-1.62
-	½	1½	-½	1½	1½	-½	8334.45	-0.3	-1.62
-	½	2½	½	1½	2½	½	8402.76	2.6	-1.62
-	½	2½	-½	1½	2½	-½	8424.36	0.4	-1.62
Parallel polarisation (π)									
-	1½	-2½	½	1½	-2½	½	13833.37	1.0	-0.943
-	1½	-2½	-½	1½	-2½	-½	13867.59	0.9	-0.943
-	1½	-1½	½	1½	-1½	½	13933.04	0.8	-0.943
-	1½	-1½	-½	1½	-1½	-½	13967.96	1.4	-0.943
-	1½	-½	½	1½	-½	½	14033.61	1.2	-0.943
-	1½	-½	-½	1½	-½	-½	14067.83	1.1	-0.943
-	1½	½	½	1½	½	½	14133.67	0.9	-0.943
-	1½	½	-½	1½	½	-½	14168.00	0.9	-0.943
-	1½	1½	½	1½	1½	½	14234.44	1.2	-0.943
-	1½	1½	-½	1½	1½	-½	14268.97	1.3	-0.943
-	1½	2½	½	1½	2½	½	14335.51	1.5	-0.943
-	1½	2½	-½	1½	2½	-½	14370.25	1.9	-0.943

for the electron spin *g*-factor, g_S, of 2.001946(13) is now in good agreement with that determined by Van Herpen *et al.* and much closer to the value expected from ab initio calculations (*19*). The parameter values for ^{16}OH given in Table III were then scaled to give the corresponding values for ^{17}OH. These values are given in Table IV (for parameters constrained in the fit of the ^{17}OH data) and in Table V (for parameters determined in the fit).

The quality of the fit is quite satisfactory as can be judged from the residuals given in Table II. The standard deviation of the fit relative to experimental error was 1.94, which is acceptably close to unity. The parameter values determined in the fit are given in the lower part of Table IV. It can be seen that all the ^{17}O hyperfine parameters have been determined.

4. DISCUSSION

In this paper, we report the observation by far-infrared LMR of rotational transitions in ^{17}OH in natural abundance (0.037%). This statement in itself is an impressive testimony to the sensitivity of the experimental technique. For the lines shown in Fig. 2, for example, we estimate a signal-to-noise ratio of 12:1 with an output time constant of 300 msec. Taking into account the nuclear spin of ^{17}O ($I = \frac{5}{2}$), the signal-to-noise for the corresponding transition in ^{16}OH would therefore be 2×10^5 to 1.

TABLE III

Revised Molecular Parameters for ^{16}OH in the $v = 0$ Level of the $X^2\Pi$ State (in MHz Where Appropriate)

$\tilde{A}$	-4168640.50(8)[a]	A_D	0.0[b]
$\tilde{\gamma}$	-3573.6(2)	γ_D	0.711(19)
B	555661.52(4)	D	57.2266(35)
$10^2 H$	0.4355[b,c]		
p	7053.10123(78)	q	-1159.9943(11)
p_D	-1.55048(13)	q_D	0.441951(24)
$10^3 p_H$	0.1577(27)	$10^4 q_H$	-0.8151(30)
a	86.1101(28)	$10c_I$	-0.9945(81)
b_F	-73.2516(68)	$10^2 c_I'$	0.6438(17)
c	130.641(14)	$10d_D$	-0.2276(14)
d	56.6837(25)		
g_L'	1.000872(5)	$10^3 g_r$	-0.6452(46)
g_S	2.001946(13)	$10^2 g_l'$	0.64146(16)
$10^2 g_l$	0.3464(65)	$10^2 g_r e'$	0.20463(12)

[a] The numbers in parentheses represent 1 standard deviation of the least-squares fit, in units of the last quoted decimal place.

[b] Parameter constrained to this value in the least-squares fit.

[c] Slightly revised value for H, obtained from recent fit of high J data for OH (20).

The measurements have been used to determine molecular parameters for ^{17}OH, including the first complete determination of the magnetic hyperfine parameters. The rotational and fine structure parameters which have been determined are given in Table V together with the values estimated from those of ^{16}OH by isotopic scaling for comparison. The reasonably good agreement for these two sets of numbers gives one confidence in the procedure used for estimating the other parameters for ^{17}OH which were constrained in the fit. Of the nuclear hyperfine parameters, only one has been determined previously, namely d for which Ehrenstein obtained a value of -415.3 ± 2.0 MHz (*8*) compared with the present value of -429.25 ± 0.67 MHz. It is of course disappointing that we have not been able to exploit the intrinsically high quality

TABLE IV

Parameters for ^{17}OH in the $v = 0$ Level of the $X^2\Pi$ State[a]

(A) Parameter values constrained in the least-squares fit.				
	10^2H	0.4309	γ_D	0.7060
	p_D	-1.53964	q_D	0.437324
	10^3p_H	0.15608	10^4q_H	-0.80374
^1H	a	86.1101		
	b_F	-73.2516	^{17}O eq_0Q	-1.92 [d]
	c	130.641		
	d	56.6837		
	g_L'	1.000869	10^3g_r	-0.6429
	g_S	2.001946	$10^2g_l'$	0.64146
	10^2g_l	0.3464	$10^2g_r{}^{e'}$	0.20391
(B) Parameter values determined in the least-squares fit.				
	$\tilde{A}$ [b]	-4168642.3(17) [c]	a	-320.7(11)
	$\tilde{\gamma}$ [b]	-3563.41(75)	b_F	-51.17(43)
	B	553734.70(21)	^{17}O c	220.8(39)
	D	56.661(19)	d	-429.49(61)
	p	7024.06(76)	eq_2Q	66(9)
	q	-1151.16(12)		

[a] Values in MHz, where appropriate.

[b] Effective parameter. The fit was performed with the parameter A_D constrained to zero.

[c] The numbers in parentheses represent one standard deviation of the least-squares fit, in units of the last quoted decimal place.

[d] Obtained from a preliminary fit of the microwave data (10).

of the microwave measurements (*10*) in our fit. It is perhaps worth noting that the parameter set given in Table IV reproduces the lambda-doubling frequencies for the $J = \frac{3}{2}$ level in Ref. (*10*) very well. However, the $\frac{5}{2}$ frequencies are only moderately well predicted and the $J = \frac{1}{2}$ frequencies do not seem to correspond at all. While a question hangs over the assignment of these lines, it is just conceivable that there is some higher-order hyperfine interaction involving the ^{17}O nucleus which would bring the two data sets into consistency. Clearly, if the published frequencies for ^{17}OH are substantiated in the reinvestigation which is currently under way (*13*), such an explanation becomes more convincing.

TABLE V

Comparison of Experimentally Determined Parameters for ^{17}OH with Those Calculated from ^{16}OH

Parameter [a]	Experimental	Calculated
$\tilde{A}$	-4168642.3(17) [b]	-4168647.4 [c]
$\tilde{\gamma}$	-3563.41(75) [b]	-3561.39 [d]
B	553734.70(21)	553734.48 [e]
D	56.661(19)	56.827
p	7024.06(76)	7028.4036
q	-1151.16(12)	-1151.884

[a] Values in MHz.

[b] Effective parameter (A_D constrained to zero).

[c] Calculated using A_D = -21.39 MHz (26), α_A = 7870 MHz for ^{16}OH (28).

[d] Calculated using γ = -3493.5 MHz for ^{16}OH (26).

[e] Calculated using α_e = 21647.4 MHz, γ_e = 177.2 MHz for ^{16}OH (27).

Perhaps the most interesting result to emerge from our study is the set of magnetic hyperfine parameters for ^{17}O. These in turn can be related to well-known expectation values over the electronic wavefunction for OH in the $v = 0$ level of its $X^2\Pi$ state (*21*). The values obtained are given in Table VI, along with estimates from other sources. The values from the EPR study are derived from a partial experimental determination of the hyperfine structure combined with an assumption that the wavefunction has the angular dependence of a $2p$ atomic orbital on the O atom. The extent to which these two sets of numbers disagree is a measure of the unreliability of this assumption since the EPR measurements are also included in the present fit. The other two sets of numbers in Table VI are the results of ab initio calculations. The first, by Cade and Huo (*22*), is based on a restricted Hartree–Fock wavefunction. In view of its simplicity, this calculation gives results which are really quite good (although the Fermi contact interaction is never reliably predicted in such a calculation). The last column in Table VI gives the results of a very recent calculation by Kristiansen and Veseth (*23*) who used the optimized basis set of Cade and Huo (*22*) and the many-body perturbation theory. The discrepancy between theory and experiment for these latest calculations is not much larger than the experimental error and gives some idea of just how good state-of-the-art calculations are for light molecules. It should be noted

TABLE VI

Values for ^{17}O Magnetic Hyperfine Parameters (in MHz) and Related Expectation Values (in m^{-3}) in ^{17}OH

Parameter	Present work	EPR (9)	Cade and Huo (22)	Kristiansen and Veseth (23)
a	-320.7(11)	-293.3	-336.2	-322.50
b_F	-51.17(43)	-86.0	0.0	-38.76
c	220.8(39)	205.8	197.7	209.65
d	-429.49(61)	-411.6	-398.7	-435.89
$10^{-31}\langle 1/r^3\rangle_\ell$	2.996	2.74	3.14	3.012
$10^{-31}\langle 1/r^3\rangle_s$	3.320	3.21	3.14	3.415
$10^{-29}\psi(0)^2$	5.699	9.58	0.0	4.317
$10^{-31}\langle(3\cos^2\theta-1)/r^3\rangle_s$	-1.373	-1.28	-1.23	-1.304
$10^{-31}\langle\sin^2\theta/r^3\rangle_s$	2.671	2.56	2.48	2.711

that, even for these calculations, it is rather hard to calculate the Fermi contact parameter b_F reliably.

By taking suitable combinations of the ^{17}O hyperfine parameters, it is possible to make independent estimates for the electron spin and orbital distributions, $\langle r^{-3}\rangle_s$ and $\langle r^{-3}\rangle_l$, in the neighborhood of the O nucleus. We find the ratio $\langle r^{-3}\rangle_s/\langle r^{-3}\rangle_l$ to be 1.108 (±0.010), a value which is well reproduced by the Kristiansen and Veseth calculation (*23*). The value is also very similar to that of 1.13 determined by Harvey for the O atom itself (*24*). The corresponding ratio for the proton in OH was determined earlier by Radford (*25*) to be $\langle r^{-3}\rangle_s/\langle r^{-3}\rangle_l = 1.174$, which, though quite similar, is significantly different.

Finally, we consider the nuclear electric quadrupole interaction in ^{17}OH. There are two parameters for a molecule in a $^2\Pi$ state,

$$eq_0Q = eQ2\langle\Lambda = \pm 1|T^2_0(\nabla\mathbf{E})|\Lambda = \pm 1\rangle \tag{2}$$

and

$$eq_2Q = eQ2\sqrt{6}\langle\Lambda = \pm 1|T^2_{\pm 2}(\nabla\mathbf{E})|\Lambda = \mp 1\rangle. \tag{3}$$

For ^{17}OH, the value for eq_0Q has been calculated by Carrington and Lucas (*9*) from the wavefunction of Cade and Huo (*22*) to be −2.6 MHz, in agreement with the value of −1.92 MHz used in our fit. The interesting feature of this calculation is that the electric field gradient at ^{17}O along the internuclear axis arises primarily from the charge

on the proton; the electronic contribution is close to zero. By contrast, the parameter eq_2Q depends only on the electron distribution around the nucleus. Even more specifically, it is a measure of the π-electron distribution only and is consequently rather more straightforward to interpret. Let us assume that the π molecular orbitals in OH are simply $2p_x$ and $2p_y$ orbitals on the oxygen atom. We can then estimate the value for eq_2Q using the electric quadrupole parameter from atomic ^{17}O. Using the experimental values determined by Harvey (*24*), it is possible to show that the axial electric quadrupole coupling constant for one electron in a $2p$ orbital on ^{17}O is

$$eq_0Q\,(\text{atom}) = 20.876(60)\ \text{MHz}.$$

The molecular parameter eq_2Q is related to this by

$$eq_2Q = \mp 3eq_0Q\,(\text{atom}) \tag{4}$$

where the upper sign refers to a $(2p\pi)^1$ configuration and the lower to $(2p\pi)^3$. On this basis, the parameter eq_2Q is estimated to be +62.6 MHz, in excellent agreement with the value determined in our analysis of 66(9) MHz. It can thus be concluded that, from the point of view of charge distribution, the π orbitals in OH are well described by atomic p orbitals, a fact which is confirmed by the Cade and Huo wavefunctions (*22*).

ACKNOWLEDGMENTS

We thank Carl Gottlieb and Harry Radford for several helpful discussions on the microwave spectrum of ^{17}OH. We are also grateful to the Science and Engineering Research Council for its support to one of us (E.R.C.).

RECEIVED: September 19, 1986

REFERENCES

1. B. E. TURNER, *Astrophys. J.* **186,** 357–395 (1973).
2. C. N. HEWITT AND R. M. HARRISON, *Atmos. Environ.* **19,** 545–554 (1985).
3. G. C. DOUSMANIS, T. M. SANDERS, AND C. H. TOWNES, *Phys. Rev.* **100,** 1735–1754 (1955).
4. G. A. BLAKE, J. FARHOOMAND, AND H. M. PICKETT, *J. Mol. Spectrosc.* **115,** 226–228 (1986).
5. J. M. BROWN, L. R. ZINK, D. A. JENNINGS, K. M. EVENSON, A. HINZ, AND I. G. NOLT, *Astrophys. J.* **307,** 410–413 (1986).
6. J. M. BROWN, J. E. SCHUBERT, C. E. BROWN, J. S. GEIGER, AND D. R. SMITH, *J. Mol. Spectrosc.* **114,** 185–196 (1985).
7. E. R. COMBEN, J. M. BROWN, T. C. STEIMLE, K. R. LEOPOLD, AND K. M. EVENSON, *Astrophys. J.* **305,** 513–517 (1986).
8. G. EHRENSTEIN, *Phys. Rev.* **130,** 669–675 (1963).
9. A. CARRINGTON AND N. J. D. LUCAS, *Proc. R. Soc. London, Ser. A* **314,** 567–583 (1970).
10. C. A. GOTTLIEB, H. E. RADFORD, AND B. P. SMITH, unpublished results (1974), *in* R. A. BEAUDET AND R. L. POYNTER, *J. Phys. Chem. Ref. Data* 7, 311–362 (1978).
11. F. F. GARDNER AND J. B. WHITEOAK, *Mon. Not. R. Astron. Soc.* **176,** 57P–60P (1976).
12. I. E. VALTZ AND V. A. SOGLASNOVA, *Astrophys. Lett.* **13,** 23–24 (1973).
13. C. A. GOTTLIEB AND H. E. RADFORD, private communication from the Center for Astrophysics, Harvard College Observatory, Cambridge, MA 02138.
14. T. J. SEARS, P. R. BUNKER, A. R. W. MCKELLAR, K. M. EVENSON, D. A. JENNINGS, AND J. M. BROWN, *J. Chem. Phys.* **77,** 5348–5362 (1982).

15. M. INGUSCIO, G. MORUZZI, K. M. EVENSON, AND D. A. JENNINGS, *J. Appl. Phys.* **60,** R161–R192 (1986).
16. J. M. BROWN, M. KAISE, C. M. L. KERR, AND D. J. MILTON, *Mol. Phys.* **36,** 553–582 (1978).
17. J. M. BROWN, C. M. L. KERR, F. D. WAYNE, K. M. EVENSON, AND H. E. RADFORD, *J. Mol. Spectrosc.* **86,** 544–554 (1981).
18. J. M. BROWN, E. A. COLBOURN, J. K. G. WATSON, AND F. D. WAYNE, *J. Mol. Spectrosc.* **74,** 294–318 (1979).
19. W. M. VAN HERPEN, W. L. MEERTS, AND L. VESETH, *Chem. Phys. Lett.* **120,** 247–251 (1985).
20. E. R. COMBEN, D.Phil. thesis, Oxford University, 1986.
21. R. A. FROSCH AND H. M. FOLEY, *Phys. Rev.* **88,** 1337–1349 (1952).
22. P. CADE AND W. M. HUO, *J. Chem. Phys.* **47,** 614–648 (1967).
23. P. KRISTIANSEN AND L. VESETH, *J. Chem. Phys.* **84,** 6336–6344 (1986).
24. J. S. M. HARVEY, *Proc. R. Soc. London, Ser. A* **285,** 581–596 (1965).
25. H. E. RADFORD, *Phys. Rev.* **126,** 1035–1045 (1962).
26. J. M. BROWN AND J. E. SCHUBERT, *J. Mol. Spectrosc.* **95,** 194–212 (1982).
27. J. A. COXON, *Canad. J. Phys.* **58,** 933–949 (1980).
28. T. AMANO, *J. Mol. Spectrosc.* **103,** 436–454 (1984).